

## Investigation on DSMC by using pareto set through fuzzy boundary impact

Iman Ashkani

MSc in Mechanical Engineering, Applied Design Trends, Guilan University  
[ashkaniiman@gmail.com](mailto:ashkaniiman@gmail.com)

**Abstract:** This study develops to employ time-varying boundary layer thickness in order to obtain optimum results for Decouple Sliding-Mode Controllers (DSMC) from the point of view of settling time and declining tracking-error. Sliding-mode controllers based on a time varying boundary layer thickness are more preferable to the fixed-boundary layer method for tracking. All the Sliding-mode controllers contain two principal and cardinal sections. The first section is the reaching mode or reaching condition, which is also called nonsliding mode. The second section is the sliding condition in which the trajectory essentially tends to the origin of the phase plane. The variation of Pareto-set achievements, which contrast each other, leads to selecting the best results from this Pareto front.

[Iman Ashkani. **Investigation on DSMC by using pareto set through fuzzy boundary impact.** *Researcher* 2014;6(7):77-92]. (ISSN: 1553-9865). <http://www.sciencepub.net/researcher>. 10

**Key words:** Boundary layer thickness; Fuzzy Logic; Genetic Algorithm; NSGA-II

### 1. Introduction:

SMC has been developed in to a general design. These controllers are examined and employed for a wide variety of systems, which contain nonlinear systems in engineering and industry. Emelyanov introduced sliding mode control, first named as Variable Structure Control (VSC). Phillipov et al. have established a systematic mathematical theory for differential equation by discontinuities. In order to reduce and decline the chattering, satisfying the reaching condition Direct approach, Lyapanov Function approach, Reaching Low Approach and the continuation Approach are pointed out in other studies. The initial inspiration of sliding-mode was essentially illustrated by a form of second-order system. The trends of the entire sliding mode are similarity of these controllers. Besides, the ambitions of SMC have been extended from stabilization to other control functions literally.

It is obvious in sliding-mode controller that, the system trajectory slides due to a sliding surface essentially. In order to overcome the system, parameter variations and noise disturbances sensitivity in the SMC during reaching phase, several researchers have applied successful methods such as high-gain performance [1]. Among the shortening of this approach is producing chattering due to sliding condition. Therefore, successful Moving Switching Surface (MSS) method has been employed for this depletion [2-4]. Using the MSS, the system sensitivity to uncertainties is remarkably reduced due to shortening the reaching phase. The benefit of this technique is that once the system state turns up a sliding surface, the system dynamics remains insensitive to a class of parameter uncertainties and disturbances.

In the sliding-mode controller, input of control must satisfy the sliding condition and stability of the trajectory on the sliding surface [5], [6]. Due to this point, the gain in SMC is applied to satisfy the system robustness and stability of the control system.

In this case, an intermediate-variable is employed to transfer the dynamic variations to couple the whole system. After all, information from the secondary objective conditions the main target, which in turn generates a control action to make both subsystems move toward their sliding surfaces [2-4]. In fact, this is only a base surface from the definition of sliding mode controller's point of view. The sliding surface equation illustrates that another surface is obviously Moving Switching Surface (MSS) behavior in the phase plane. Therefore, the boundary layer thickness is designed upon the Moving Switching Surface in order to reduce the chattering during the motion of the surface. Actually, the time varying boundary layer thickness is more preferable than constant for tracking [5].

Fuzzy Logic Controller was developed by Mamdani in order to satisfy Zadeh's theory [8]. In fact, this Fuzzy inference system was proposed as the first attempt to control a steam engine and boiler system using a set of linguistic control rules. Mamdani's FLC was accomplished from experienced human operator's knowledge. Nowadays, fuzzy system has been utilized to a broad variety of courses ranging from control; signal processing, integrated circuit, communications, manufacturing, and expert systems to business, management, medicine, psychology, etc. However, there are innumerable most significant applications of fuzzy systems in different courses. The downside of FLC is that there is no systematic strategy in order to design them.

Obviously, designing FLCs based on expert knowledge is a boring and time consuming process. In order to design the fuzzy sets, the rule bases has been well documented by using artificial neural networks (ANN's) [9-10], and genetic algorithm (GA's) [12-19].

Optimization in engineering field has always been of great prominence and pursuit particularly solving complex real world design problems. Essentially, the optimization process is established to find a set of values of an objective or cost function. There are several calculus-based techniques containing gradient approaches to single objective optimization which are well documented in [21, 22]. In these troubles, there are several objective or cost functions (a vector of objectives) to be optimized (minimized or maximized). Their objectives often contrast each other so that improving one of them will degenerate another. Hence, there is no separate optimal solution as the best with respect to all the objectives or Pareto set [28, 33] for multi-objective optimization problems (MOP's).

**2. Moving Switching Surface**

During the sliding mode control process, the system has invariance properties yielding disturbances and variations. One of the most important preoccupations in SMC is that reaching condition due to the switching surface is ensured. In general, the more robust systems include the short time reaching phase. The prevalent switching surfaces in the sliding mode control are always very far and independent of initial conditions. These typical switching surfaces may be sensitive to parameter variations and extraneous disturbances during the reaching phase. One of the most powerful methods in order to decrease and eliminate the reaching time is High-Gain strategy which was introduced in [1]. Nevertheless, extreme sensitivity to unmodelled dynamics and higher chattering is the drawback of this strategy. Trying to overcome this disease, Moving Switching Surface was established. The representative point of the system is constrained to move along a predetermined switching surface. Therefore, the design of the switching surface completely determines the performance of the system. Hence, because of applying this method, the robustness of the controller can be improved by shortening the time required to attain the sliding mode or may be assured during whole intervals of control action. For this purpose, the surface is initially designed to pass the initial conditions and is subsequently moved towards a predetermined switching surface by shifting or rotating. Consequently, after each movement of the sliding surface, the system characteristic point is no longer

on the surface, and the system is not insensitive to parameter uncertainties and disturbances [2-4]. Fig.1 illustrates the details of the sliding condition during the motion of the MSS in the phase plane. Hence, during the moving surface the trajectory slides due to the sliding surface. In general, (1) describes the type of MSS behavior in the phase plane.

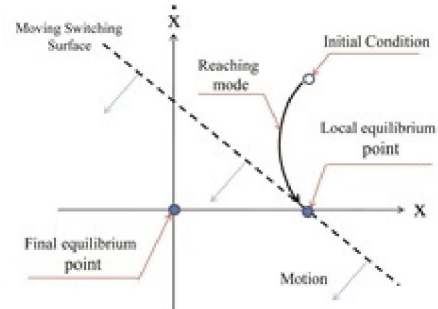


Fig.1. MSS performance

$$S(x, t) = \Xi(x, \tau) \cdot \dot{\tilde{x}} + C\tilde{x} + \Lambda(x, \tau) \quad ,$$

$$(t_0 < t < t_{Final}), (t_{Start} < \tau < t_{Stop})$$

$$(\tilde{x}(t) = x(t) - x_d(t)) \quad (1)$$

Where  $\Xi, \Lambda$  are time-varying functions or Step functions [2, 4]. Therefore, it is leading the surface to be as an MSS or SSS behavior surface in the phase plane.  $t_0$  is start of the dynamic system trajectory and  $t_{Final}$  is the time when the dynamic trajectory is stabled at equilibrium point.  $\tau$  is the time duration of MSS motion and  $t_{Start}$  and  $t_{Stop}$  are the starting and stopping times of MSS motion in the phase plane, respectively. However, by selecting the appropriate functions, it can be guaranteed during the sliding condition such as rotating or shifting motion.

**3. Fuzzy systems**

The Fuzzy Logic Controller, whose structure is based on human knowledge, is established on IF-THEN rules. On the other hand, fuzzy systems are multi-input/single-output conversion, from a real-value vector to a real-valued scalar which is established on human knowledge. Through this description, consider a human operation system like automobile. In order to have a safe riding; the operator tries to respect safe rules. For instance, if the car drives extremely fast, the operator attempts to dispile the following rule.

IF *the speed is high*, THEN *apply less force to accelerator*

In order to convert the FLC with respect to

human knowledge, it is necessary to restructure the fuzzy system mathematically. In fact, any fuzzy system includes two principle sections. The first section is named fuzzy controller, containing fuzzy structure or fuzzy logic process which is established based on the mathematical knowledge. The second part is the fuzzy operation, which is impressive of human knowledge or human expert to conduct the most successful orders.

**3.1. Fuzzy structure and definitions**

Consider  $U$  is the universe of discourse, or universal set, which contains all the possible elements of concern in each particular context or application generally. A classical (crisp) set  $A$ , or simply a set  $A$ , is recalled in the universe of discourse.  $U$  is able to be defined by listing all of its members (the list method) or by specifying the possessions that must be satisfied by the members of the set.

*Definition.1.* A fuzzy set is characterized in a universe of discourse  $U$  by membership function  $\mu_A(x)$  that takes values in the interval  $[0, 1]$ .

Thus, a fuzzy set is a generation of a classical set by permitting the membership function to take any value in the range  $[0, 1]$ . In other words, the membership function of a classical set is only able to take values-Zero and One; nevertheless, the membership function of a Fuzzy set includes a continuous function with range  $[0, 1]$ . For instance,

$$(2) \mu_A(x) = \begin{cases} \left(1 - \frac{|x_1 - x_1^*|}{b_1}\right) \otimes \dots \otimes \left(1 - \frac{|x_n - x_n^*|}{b_n}\right) & \text{if } |x_i - x_i^*| \leq b_i, i = 1, 2, \dots, n \\ 0 & \text{Otherwise} \end{cases}$$

Equ (2), illustrates the *triangular fuzzifier*, where  $b_i$  are positive parameters and the t-norm  $\otimes$  is usually chosen as *algebraic product* or *min product*. In this paper, *triangular fuzzifier* and *min* t-norm have been used [31].

**3.1.2. Fuzzy inference engine**

In a Fuzzy inference engine, Fuzzy logic principles are employed to mix the Fuzzy IF-THEN rules in the Fuzzy rule base in to a converting from a Fuzzy set  $A'$  in  $U$  to a Fuzzy set  $B'$  in  $V$ . A Fuzzy IF-THEN rule is translated as a Fuzzy relation in the input-output product space  $U \times V$ . In fact, any practical fuzzy rule base constitutes more than one rule. In order to infer the set of rules, two main ways are employed, composition based inference and individual-rule based inference. According to these methods, there are a variety of options in the fuzzy

consider  $\mu_y$  which represents age youth and  $\mu_o$  which points to age old of human life membership functions.

$$\begin{cases} \mu_y(x) = y(x) \\ \mu_o(x) = o(x) \end{cases}$$

Thus, a human with 30 years of age, has the  $\mu_y(30) = 0.75$  similarly  $\mu_o(30) = 0.25$ . Which illustrates the fact that human with 30 years of age is young with 0.75 degree of youth and the same is old with 0.25 degree of old, age style.

**3.1.1. Fuzzifiers**

Consider the set of universe of discourses  $U = \prod_{i=1}^n U_i$ , The *fuzzifier* is defined as a conversion from a real-valued point  $x^* \in U \subset R^n$  to a fuzzy set  $A'$  in  $U$ . In fact, fuzzifier converts the crisp input to a linguistic variable using the membership functions stored in the fuzzy knowledge base. Fuzzifier should respect the fact that the input has large membership value at  $x^*$ ; that is the fuzzy set  $A'$  should have major membership value at  $x^*$ . The most applicant fuzzifiers are *Singleton fuzzifier*, *Gaussian fuzzifier* and *Triangular fuzzifier*.

inference engine. *product*, *Mamdani* or *Gödel*, *Dienes-Rescher*, *minimum inference*, *Lukasiewicz* and *Zadeh inference engine* strategies are principal product inferences [31]. (3) illustrates the *minimum inference engine* and Fig. 2 demonstrates and describes the performance of *min inference engine*.

$$(3) \mu_{B'}(y) = \max_{l=1}^M \left[ \sup_{x \in U} \min(\mu_{A'}(x), \mu_{A_1}(x_1), \dots, \mu_{A_n}(x_n), \mu_{B'}(y)) \right]$$

Where  $A_1, A_2, \dots, A_n$  given fuzzy set  $A'$  in  $U$ , gives the fuzzy set  $B'$  in  $V$ . The product inference engine and the minimum inference engine which have been employed in this paper are the most commonly used fuzzy inference engines in fuzzy systems and fuzzy control. Their main advantage is their computational simplicity.

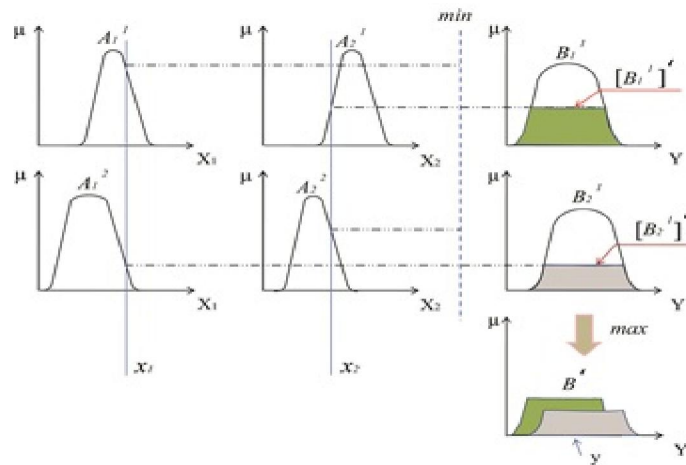


Fig.2. Output membership function using *min inference engine*

3.1.3. Fuzzy Rule Base structure

A fuzzy rule base comprises a set of fuzzy IF-THEN rules. In fact, it is the heart of the fuzzy system in the sense that all other parts are employed to implement these rules in a reasonable and efficient manner. Particularly, the fuzzy rule base is composed as follows.

$$(4) R(u)^l : \text{IF } x_1 \text{ is } A_1^l \text{ and...and } x_n \text{ is } A_n^l, \text{ THEN } y \text{ is } B^l$$

Where  $A_i^l$  and  $B^l$  are fuzzy sets which  $U_i \in R$  and  $V \subset R$ , respectively, and  $(x_1, x_2, \dots, x_n)^T \in U$  and  $y \in V$  are the input and output (linguistic) variables of fuzzy systems, respectively.

*Definition.2.* A set of fuzzy is complete IF-THEN rules, if for any  $x \in U$ , there exists at least one rule in the fuzzy rule base, any rule  $R_u^{(l)}$  (in the form of (18)), such  $\mu_{A_i^l}(x_i) \neq 0$  for all  $i = 1, 2, \dots, n$ .

Definition 2 explains that at any point in the input space, there is at least one rule that "fires". For instance, consider 2-input-1-output fuzzy system with,  $U = U_1 \times U_2 = [0,1] \times [0,1]$  and  $V = [0,1]$ . By definition of  $M_1, S_1$  and  $L_1$  in  $U_1$ , and two fuzzy sets  $S_2$  and  $L_2$  in  $U_2$  are shown in Fig.3. In order for a fuzzy rule base to be complete, it must include the following rules whose IF parts constitute all the possible combinations of  $S_1, M_1, L_1$  with  $S_2, L_2$ .

$$R(u)^1 : \text{IF } x_1 \text{ is } S_1 \text{ and } x_2 \text{ is } S_2, \text{ THEN } y \text{ is } B^1$$

$$R(u)^2 : \text{IF } x_1 \text{ is } S_1 \text{ and } x_2 \text{ is } L_2, \text{ THEN } y \text{ is } B^2$$

...

$$R(u)^6 : \text{IF } x_1 \text{ is } L_1 \text{ and } x_2 \text{ is } L_2, \text{ THEN } y \text{ is } B^6$$

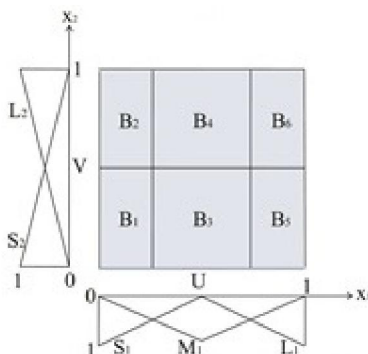


Fig. 3. Two-input fuzzy rule table

3.1.4. Defuzzifier

The defuzzifier is defined as a conversion from fuzzy set  $B^l$  in  $V \subset R$  (that is the output of the fuzzy inference engine) to crisp point  $y^* \in V$ . This means Defuzzifier converts the fuzzy output of the inference engine to crisp using membership functions analogous to the ones used by the Fuzzifier. Three main defuzzifications are Center of gravity Defuzzifier, Center average Defuzzifier and Maximum Defuzzifier. In this paper, we have exploited Center of gravity Defuzzifier method. The main advantage of Center of gravity defuzzifier lies in

its intuitive plausibility. Fig.4 implies the Center of gravity performance.

$$y^* = \int_v y \mu_{B'}(y) dy / \int_v \mu_{B'}(y) dy \quad (5)$$

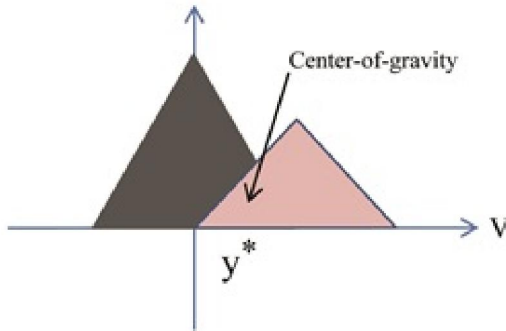


Fig. 4. Center of gravity performance

**3.2. Fuzzy operation system**

With regard to fuzzy logic controller applications which are established on human knowledge, the components of these systems must be restructured. In fact, quality of the fuzzy controller design conducted to successful process [29]. For this purpose, the components of the FLC such as the membership functions, and applying the appropriate rule-bases must be design. The FLC pioneers and former researchers originally were used to construct the FLCs by expressing expert knowledge from a human operator in terms of fuzzy linguistic rules, and after that the controller was tuned by trial-and-error. In accordance with large amount of number of fuzzy components, it was an extremely boring and time consuming process. Hence, the GAs strategy was employed to overcome this disease. Thus, in every FLC, the purpose is trying to decline FLC parameters. As we know, there is no systematic method in order to design the FLCs. So, the drawback of this controller leads the researchers to invent several methods [30, 31]. For this purpose, the fewest of the parameters are employed in order to restructure of FLC. [32]

**3.2.1. Design of membership functions**

Assemblage of a fuzzy controller is accomplished by the perseverance of some parameters which include the numbers and center values of the input and output membership functions, and linguistic control rules. Fig.13 illustrates the spartan structure and the design parameters of the Fuzzy Controller with triangular shape membership functions. The distance between the zero and the center value is defined by considering linguistic value of one. Our first commotion stems from the point that membership functions are strange number in general.

Fig.5 demonstrates the pattern of triangular membership functions and the position of the membership function's center, respectively.

$$x_i = (i/n)^{Ps} \quad (i = 0, \dots, n) \quad (6)$$

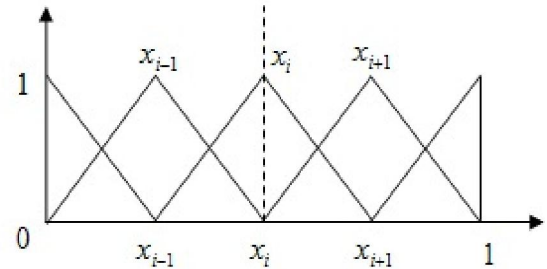


Fig. 5. Arrangement of the triangular membership function by  $Ps$  parameter

**3.2.2. Fuzzy linguistic rules base on Characteristic parameters**

In order to accomplish the fuzzy linguistic rules, it is required to exploit only a few attribute parameters needed for the construction of a rule table Fig.6 (a). Through districition of the rule table it can be divided into the several regions which have the same repercussions. The number of these divided-suburbs corresponds to the number of output membership functions. The divided suburbs have been arranged with some guidelines as one of the membership functions. By perceiving a phase plane of input-1 and input-2, the descendant between the arranged divided-suburb can be straightforwardly known. Fig.6 (b) illustrates that the rule table can be characterized in the phase plane. Perceiving the divided-suburb in the rule table is able to demonstrate in the phase plane. As a consequence, the parameters' characteristic for the fuzzy linguistic rules is able to be acquired from the locations of the seed points which are determined by following the procedure for determining the center values of the membership functions (7), (8), Figs 6 (a), (b).

$$x_i = L.(i/n)^{Ps} \quad (7)$$

$$y_i = (i/n)^{Ps} . \tan(\psi) \quad i = 0, \dots, n$$

$$L = \begin{cases} \tan(\psi) & \text{If } |1/\tan(\psi)| \geq 1 \\ 1/\tan(\psi) & \text{Otherwise} \end{cases} \quad (8)$$

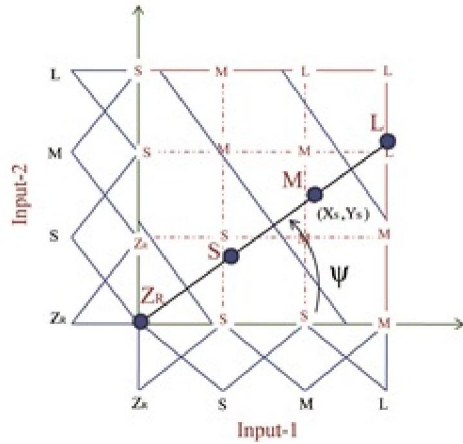


Fig.6. a. separating the rule-table with parallel seedlines; b. Rule-table base on the sections

The FLC has been depicted with a few characteristic parameters such as  $n, P_s, P_m$  and  $\psi$  is defined in the above justifications. Through this powerful strategy of FLC design, optimal FLC can easily be obtained through the optimization of the characteristic parameters.

**4. TORA system Simulation and Discussion**

The Translational Oscillations with Rotational Actuator (TORA) problem is portrayed in Fig.7. The controversial problems in this system are substantial nonlinearity and the benefits of a physically meaningful concept of energy storage. A straight rotational proof mass (with regard no gravity effect) is appended to a translating cart by instrumentation of a DC motor. The cart is fixed by a spring initially with no damping and unaccompanied actuation is through the DC motor torque. The intention of the problem is to apply the torque input to tender disturbances to the base translational mass using the proof mass. The motions of oscillations are represented in (9).

$$\begin{aligned} (M + m)\ddot{x}_c + mr(\ddot{\theta} \cos \theta - \dot{\theta}^2 \sin \theta) + kx_c &= d \\ (I + mr^2)\ddot{\theta} + m\dot{x}_c r \cos \theta &= N \end{aligned} \quad (9)$$

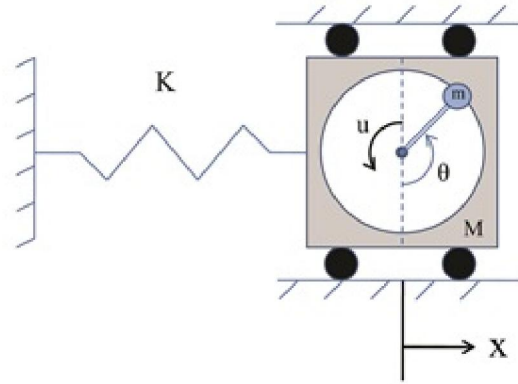


Fig.7. Portray of TORA system

Where  $M$  characterizes the both mass of the rotor and cart,  $x_c$  is translational position,  $m$  is the rotor mass,  $d$  is the disturbance force acting on the cart,  $\theta$  is the rotational angle,  $k$  is the stiffness of the linear spring,  $I$  is the moment of inertia of the mysterious mass,  $N$  illustrates the control torque exploited to proof mass, and  $r$  is the radius of rotation. After normalized transformation in the space of state variable, we can rewrite (10).

$$\begin{aligned} \dot{x}_1 &= x_2 \\ \dot{x}_2 &= -x_1 + \xi \sin x_3 + d \\ \dot{x}_3 &= x_4 \\ \dot{x}_4 &= -\frac{\xi \cos x_3}{1 - \xi^2 \cos^2 x_3} (x_1 - \xi(1 + x_4^2) \sin x_3 - d) + \frac{1}{1 - \xi^2 \cos^2 x_3} u \end{aligned} \quad (10)$$

Where  $x_1$  is cart position,  $x_2$  is cart velocity,  $x_3$  is rotor angle,  $x_4$  is rotor angular velocity and the start points are:

$$x_{1,S} = 1; x_{2,S} = 0; x_{3,S} = 0; x_{4,S} = 0.$$

And  $\xi$  is parametric uncertainty,  $0 < \xi < 1$ . In this paper, we perceive  $\xi = 0.1$ .  $d$  is external disturbance which is bounded as  $|d| \leq 0.08$ . At last,  $u$  is input torque [38]. Thus  $S_1, S_2$  are defined for the state vector of (10) as follows.

$$S_1 = C_1(\theta - Z) + \dot{\theta} = C_1(x_3 - Z) + x_4 \quad (11)$$

$$S_1 = C_2x + \dot{x} = C_2x_1 + x_2 \quad (12)$$

Which,

$$z = \text{sat}(S_2 / \varphi_2) Z_u \quad 0 < Z_u < \pi \quad (13)$$

Considering (29), the bound of repercussions of  $Z$  is upper bound of  $x_3$  in

TORA system." It has a value proportional to  $S_1$  and has the range proper to  $x_3$  [38]. The range of  $x_3$  is  $0 < x_3 < \pi$  for TORA system, Therefore, the bound of  $Z_u$  is  $0 < Z_u < \pi$ . Consequently, substituting,  $\dot{S}_1 = 0$  the input control repercussions would be (14).

$$u_{eq} = (1 - \xi^2 \cos^2 x_3)[-C_1 x_4 + \frac{\xi \cos x_3}{1 - \xi^2 \cos^2 x_3}(x_1 - \xi(1 + x_4^2) \sin x_3 - d)] - (1 - \xi^2 \cos^2 x_3) C_1 \dot{Z} \quad (14)$$

Adding the gain control to the equivalent input, it will result as the following input control.

$$u = u_{eq} - K \cdot \text{sat}(S_1/\varphi_1) \quad (15)$$

Which,  $K$  is

$$K = b^{-1} \hat{b}[F(x,t) + D(x,t) + \eta], \quad (16)$$

And for the state vector (16),  $b^{-1} = (1 - \xi^2 \cos^2 x_3)$ ,

$F(x,t) = |f(x,t) - \hat{f}(x,t)|$ , and  $x_d = 0$  as a consequence,  $\hat{f}(x,t) = 0$ .  $0 < |D(x,t)| < 0.08$ ,

plus  $\eta$  is positive constant. The FLC's time varying boundary layer thickness is utilized for the surfaces  $S_1$ ,  $S_2$ , consequently, time varying  $\varphi_1 = \varphi_1(t)$ ,  $\varphi_2 = \varphi_2(t)$  is substituted in preference to uninterrupted  $\varphi_1$ ,  $\varphi_2$ . The system is desperate for stability. *Theorem.1* illustrates that the system (10) is stable by substituting the input control (15).

**Theorem 1.** Consider the dynamic system described by (10) and Moving Switching Surface (MSS) (11) and the  $F(x,t)$  and  $D(x,t)$  are bounded, and  $\varphi_2(t)$ ,  $\dot{\varphi}_2(t)$  derived by FLC appear in  $Z$ , (Fig.7) is bounded, so with controller (15), it can guarantee the asymptotic stability of the system.

**Proof.**

Assume Lyapunov function for this procedure as (17). And differential Lyapunov is as (18).

$$V = \frac{1}{2} S_1^2 \quad (17)$$

$$\dot{V} = \dot{S}_1 S_1 \quad (18)$$

Substituting (18) in the  $\dot{S}_1$ , can be rewritten (19) as below.

$$1/b_1 [-K \cdot \text{sat}(S_1/\varphi_1)] S_1 \leq -\eta |S_1| \quad (19)$$

$$1/b_1 [-(|f(x,t)| + D(x,t) + \eta) \cdot \text{sgn}(S_1)] S_1 \leq -\eta |S_1| \quad (20)$$

Substituting (16) in (19) and concentration, out of boundary layer  $\varphi_1$ ,  $\text{sgn}()$  is substitute in preference to  $\text{sat}()$  in (19), dividing (20) on the  $|S_1|$ , (21) is

accomplished.

$$1/b_1 [-(|f(x,t)| + D(x,t) + \eta) \cdot \text{sgn}(S_1)] \cdot (S_1/|S_1|) \leq -\eta \quad (21)$$

Considering

$$S_1/|S_1| = \text{sgn}(S_1), \quad 1/b_1 [-(|f(x,t)| + D(x,t) + \eta)] \leq -\eta \quad (22)$$

As a consequence (22), and considering  $b_1$ ,  $|f(x,t)|$  and  $D(x,t)$  are positive bounded, is true.

Then (22) implies  $\dot{V}$  is negative semi-definite. So

$$\dot{V} \leq -\eta |S_1| \quad (23)$$

Therefore,  $\dot{V} = S_1 \cdot \dot{S}_1 \leq 0$ . Then, for all  $t > 0$ ,  $\dot{V} \leq 0$  holds and is a monotonous nonincrease function. Through  $\dot{V} \leq 0$ ,  $\lim_{t \rightarrow \infty} V$  exists i.e.  $V(\infty)$  exists. Then  $S_1$ , is bounded and  $\varphi_2$  is bounded, too. The negative semi definiteness of the Lyapunov function assures that  $S_1$ ,  $\varphi_2$  are bounded. Let  $\Gamma(t) = \eta |S_1| \leq -\dot{V}$  and integrate  $\Gamma(t)$  with respect to time, then yields

$$\int_0^t \Gamma(\tau) d\tau \leq \Gamma(S_1(0, \varphi_2(0), \dot{\varphi}_2(0))) - \Gamma(S_1(t, \varphi_2(t), \dot{\varphi}_2(t))) \quad (24)$$

Because  $V(S_1(0, \varphi_2(0), \dot{\varphi}_2(0)))$  is bounded, and  $V(S_1(t, \varphi_2(t), \dot{\varphi}_2(t)))$  is bounded and nonincreasing, it is demonstrated that,

$$\lim_{t \rightarrow \infty} \int_0^t \Gamma(\tau) d\tau < \infty \quad (25)$$

In addition, since  $\dot{\Gamma}(t)$  is bounded, by Barbalat's lemma [6], it can be demonstrated that  $\lim_{t \rightarrow \infty} \Gamma(t) = 0$  and  $S_1 \rightarrow 0$  as  $t \rightarrow \infty$  can be accomplished. Eventually, as a result, the control system is asymptotically stable.

### 8.1. Input FLC Gain's control

Gain control, which is an important factor in reaching condition, is exploited not only to satisfy the sliding condition, but also to guarantee the stabilization of sliding-mode control process. Some of the strategies for the gain control are demonstrated in [6]. Restructure the gain control in the time varying boundary layer to satisfy the sliding condition as illustrated in [5]. To accomplish this ambition, the input control of FLC is scribbled. Which in (26), (27)  $T$  is input FLC and  $Q$  is the derivative of FLC process respectively.

$$T = |\dot{S}_1 \text{sgn}(S_1)| \quad (26)$$

$$Q = \eta - \dot{\varphi}_1 \quad (27)$$

So, we can replace (16) with (28),

$$K = b^{-1} \hat{b} [F(x, t) + D(x, t) + Q] \quad (28)$$

In case  $S_1$  is inside the boundary layer, we replace  $T$  in (26), as (29).

$$T = K_{\max} \beta / C_1 \cdot |\text{sat}(S_1 / \varphi_1) + 1| \geq |\dot{S}_1 \text{sgn}(S_1)|$$

$$(S_1 \leq \varphi_1 \leq K_{\max} \beta / C_1) \quad (29)$$

Where,  $(\beta = (b_{\max} / b_{\min})^{1/2})$  and  $C_1$  are strictly

positive according (11).  $K_{\max}$  is a positive constant in order to satisfy the sliding condition.

8.2. Substituting FLCs in DSMC system structure

Substituting the FLCs in the TORA system structure is illustrated in Fig.8 (a). The FLCs input for the boundary layer thicknesses are the vector contains distance of the trajectory and the angles between the vector of the trajectory and the base point on the sliding surface Fig.8 (b),(c) [5].

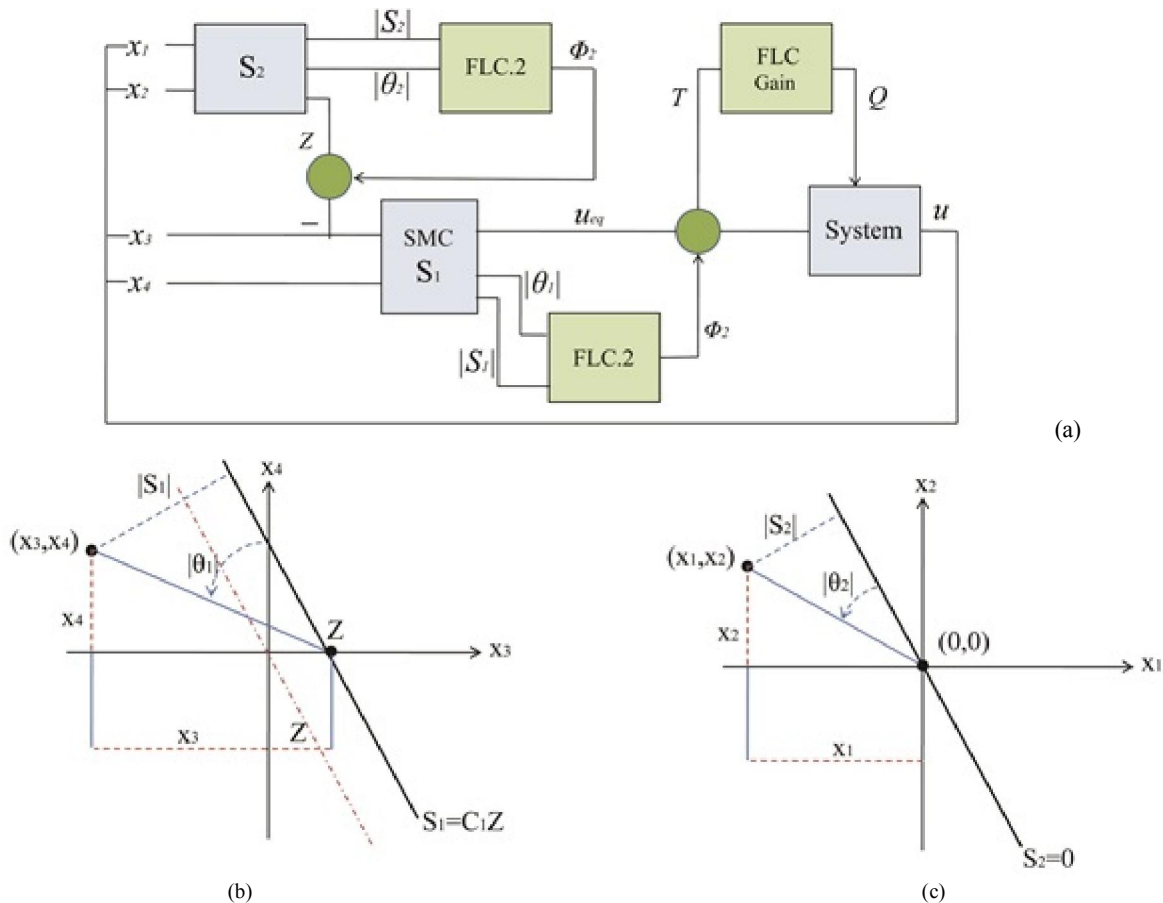


Fig.8.(a). The block of DSMC, and FLCs. (b). Vector of  $(x_3, x_4)$ , from the  $S_1 = C_1 Z$ , (c). Vector of  $(x_1, x_2)$ , from the  $S_2 = 0$

4.3. Four-objective in order to minimize Settling-time and Tracking-error of DSMC and FLCs for TORA system

As already discussed, the multi-objective optimization process is a strong strategy which is established in order to constrain vector parameters to satisfy the objective function conditions. For this purpose, in every optimization process, the parameters which are limited by constrained conditions must be selected. Due to this point, the

appropriate objective functions lead to the superior solution and results. The optimization parameters which are selected for this process are: the DSMC parameters, FLC.1 parameters (FLC for designing  $\varphi_1$ ), FLC.2 parameters (FLC for designing  $\varphi_2$ ) and FLC.Gain (FLC for designing Gain). (See Table 1)

One of the powerful, prevalent and spartan methods in multi-objective optimization is

Coefficient-Weights for coupling the cost-functions with appropriate coefficients. The proportions of the coefficients depend on the effect of the cost-function. Therefore, the Coefficient-Weights of cost functions is generally as (30),

$$F_{ws}(X) = \sum_{i=1}^n w_i f_i(x) \quad (30)$$

Where  $n$  is the multiplicity of objective functions and  $w_i$ , are the constant coefficient weights. The coefficient Weights will be chosen to satisfy,  $\sum_{i=1}^n w_i = 1$  condition. Cost-functions  $f_1, f_2$  are exploited for (30) as illustrated in (31).

$$f_1 = \int_0^t |x_1| \cdot \tau^2 d\tau, \quad f_2 = \int_0^t |x_2| \cdot \tau^2 d\tau \quad (31)$$

Where,  $x_1$  is the cart position, and  $x_2$  is the velocity of the cart in TORA system and  $t$  is crowd the range (0 - 100 (s)). As shown in equation (31), the power of  $t$  is used second degree that emphasizes the settling-time repercussions for the CART position and CART velocity. It is significant that the CART position is much more important than the CART velocity; therefore, the coefficient of the cost-functions  $f_1, f_2$  is assumed as illustrated in (32).

$$F_1 = (0.95) \cdot f_1 + (0.05) \cdot f_2 \quad (32)$$

To minimize the tracking-error of the pole-position and pole velocity, the trapezoid of the angle position and the angular velocity must be reduced. Therefore, the cost-functions  $f_3, f_4$  are defined as illustrated in (33).

$$f_1' = \int_0^t |x_3| \cdot \tau d\tau, \quad f_2' = \int_0^t |x_4| \cdot \tau d\tau \quad (33)$$

Where  $x_3$  is the POLE position, and  $x_4$  is POLE velocity of rotation actuator as scribbled, the repercussion of time in (33) is much less than (31) through in (33) the minimization of trapezoid of the tracking-error is more important; nevertheless, repercussions in (34) are much more than the time. Identically, due to selection of the appropriate coefficient as illustrated in (34), it is described that the repercussions of POLE position are much more significant. Moreover, time effective in (33) is subjected to convergence and stabilizes the POLE position.

$$F_2 = (0.9) \cdot f_1' + (0.1) \cdot f_2' \quad (34)$$

$F_1, F_2$  are defined as two main objective functions, in multi-objective optimization process;

therefore, while  $F_1$  is minimized,  $F_2$  is maximized and vice versa. It is assumed that the population size of 20 has been chosen with crossover probability  $P_C$  and mutation probability  $P_m$  equal to 0.85 and 0.1, in the multi-objective process, respectively, and considering 100 generations.

Fig.9 depicts the optimized Pareto set for two objective functions  $F_1$  and  $F_2$ . Therefore, as is a scribbled in Fig.9, these Pareto sets are opposite, when  $F_1$  is minimized,  $F_2$  is maximized. The cost function  $F_1$ , is exploited to minimize the settling time identically objective function  $F_2$ , is exploited to minimize the tracking-error, by noticing that  $x_d = 0$ , on the surface  $S_1$ , so  $\tilde{x}(t) = x(t)$ .

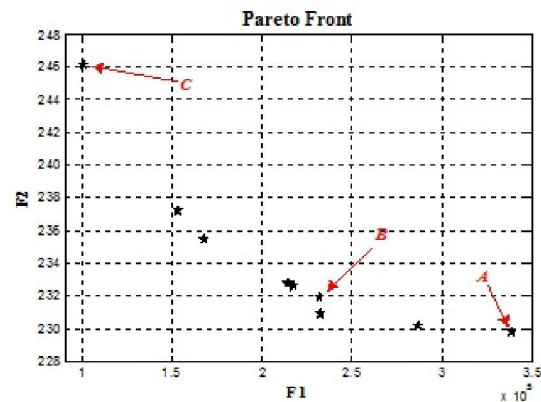


Fig.9. TORA system Pareto set of two objective functions  $F_1$  and  $F_2$

#### 4.4. The Comparison of the Pareto set $F_1$ and $F_2$

As the analogy results are demonstrated in Fig. 17, points A, B and C from the Pareto set are selected. Therefore, the fact that  $F_1$  is the addition of  $f_1$  and  $f_2$  (34) is considerably important. By alleviating the Pareto set, the settling time concentrate alleviation in the Pareto front both  $x_1$  (Cart position) and  $x_2$  (Cart velocity) must be reduced. Fig.10. (a), (b) satisfy this assumption. As illustrated in Fig.11 (a), (b), the culminations of the angular velocity in cost functions emphasize the Tracking-error in contrast to settling-time for TORA system.

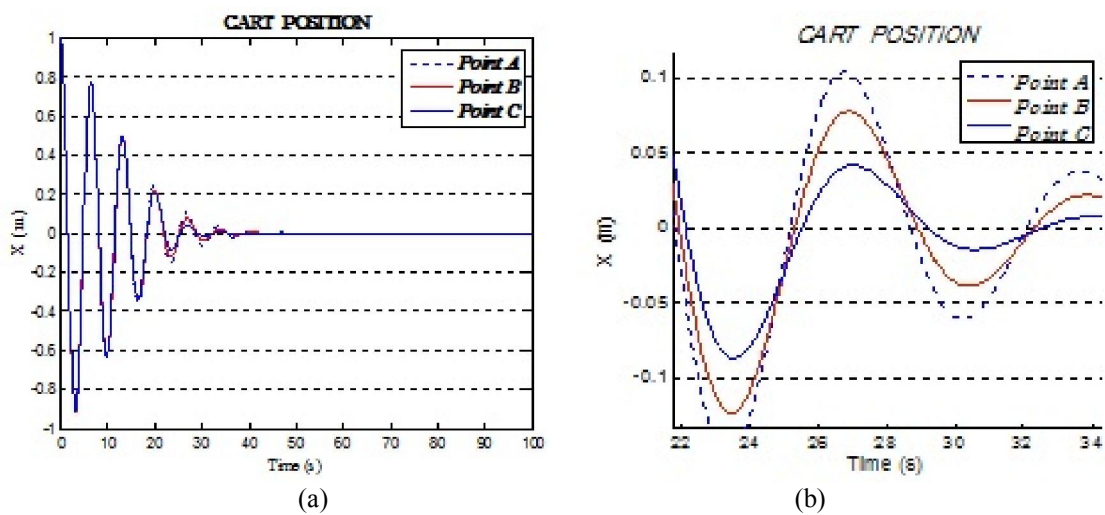


Fig.10. (a),(b). Settling time cart position point (A, B, C)

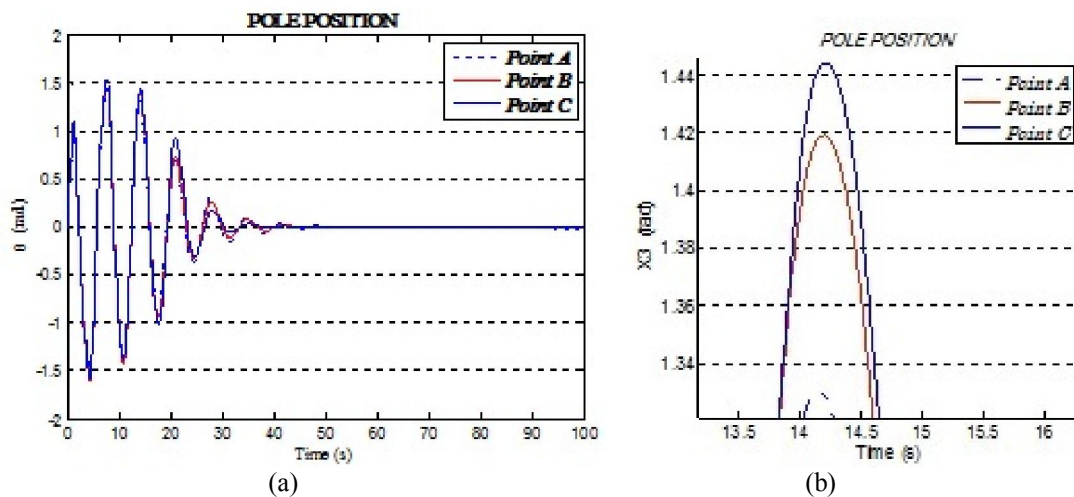


Fig.11 (a), (b). Comparison of tracking-error of angle's POLE, points A, B and C in Pareto set.

Comparing points A, B and C in Fig.10 (a), (b) transparently by alleviating the settling time in Fig.11 (a),(b) in point C the tracking-error increases,

scribbles the cost functions  $F_1, F_2$  and settling time of CART and POLE position and velocity. The results of this achievement are demonstrated in Table.2.

Table 1. Multi-Objective optimization parameters and results (point A, B and C of Pareto front) (TORA)

Control System	Parameter	Constrain	A	B	C
DSMC	$C_1$	Positive constant	0.6630	0.6630	0.6630
	$C_2$	Positive constant	8.400	8.400	8.400
	$Z_u$	$0 \leq Z_u \leq \pi$ (for TORA system)	2.068	2.18	2.18
	$K_{max}$	$(C_1 \cdot \varphi_1 / \beta) \leq K_{max}$ (Equation. (43))	7.3345	7.3345	6.9330
FLC.1 $\varphi_1$ Design	$N$	$3 \leq N$ (the number of membership functions)	5	5	5
	$P_{S,1}$	Positive constant	4.53	4.53	4.53
	$P_{S,2}$	Positive constant	4.53	4.53	4.53
	$P_{S,out}$	Positive constant	5.74	5.74	5.74
	$\psi$	$0 \leq \psi \leq \pi / 2$	1.13	1.13	1.34
FLC.2 $\varphi_2$ Design	$N$	$3 \leq N$ (the number of membership functions)	4	3	3
	$P_{S,1}$	Positive constant	0.78	1.003	1.003
	$P_{S,2}$	Positive constant	6.69	6.09	6.69
	$P_{S,out}$	Positive constant	5.71	5.51	1.04
	$\psi$ (rad)	$0 \leq \psi \leq \pi / 2$	1.24	1.31	1.17
FLC. Gain	$N$	$3 \leq N$ (the number of membership functions)	6	6	6
	$P_{S,1}$	Positive constant	5.24	5.39	5.39
	$P_{S,2}$	Positive constant	5.25	5.25	5.25

Table 2. Cost functions and comparison points of Pareto set of TORA

POINT	CART Position Settling time (s)	CART Velocity Settling time(s)	ACTUATOR Position range (rad)	ACTUATOR Velocity range (rad/s)	Cost Function F1	Cost Function F2
A	30.90	29.27	2.980	3.340	338944.1	229.77
B	27.92	28.80	3.128	3.492	231600.8	231.93
C	24.61	25.64	3.130	3.532	100504.6	246.16

Table 2, implies the settling-time of Cart Position and Cart Velocity decreases with respect to decrease of cost function  $F_1$ . On the other hand, cost function  $F_2$  emphasizes minimization of the angle position (which is  $|\theta_{max} - \theta_{min}|$ ) and angular velocity ( $|\dot{\theta}_{max} - \dot{\theta}_{min}|$ ) of rotation actuator variations and the tracking-error. Obviously, the main purpose of the TORA system control is attempting to decrease the CART position settling time. Therefore, we have

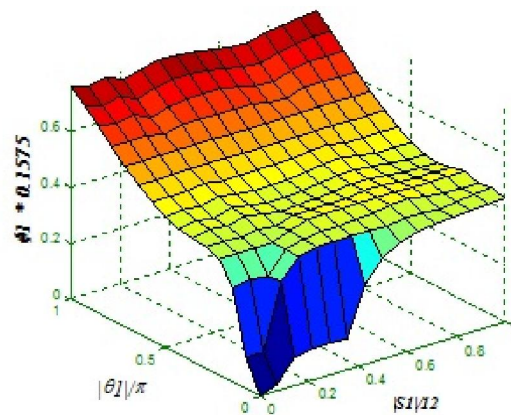
chosen point C from the Pareto set because of its minimizing the settling time.

8.5. Point C of Pareto set

As a repercussion, the parameters which are achieved from the optimization process for point C of Pareto set are as below. (See Table 1) Besides, the FLCs details are illustrated in this section.

	<i>Input</i>   $S_1$					
	Z	S	M	B	VB	
<i>Input</i>   $\theta_1$	Z	1	2	2	3	4
	S	2	2	3	3	4
	M	3	3	3	4	4
	B	4	4	4	4	4
	VB	5	5	5	5	5

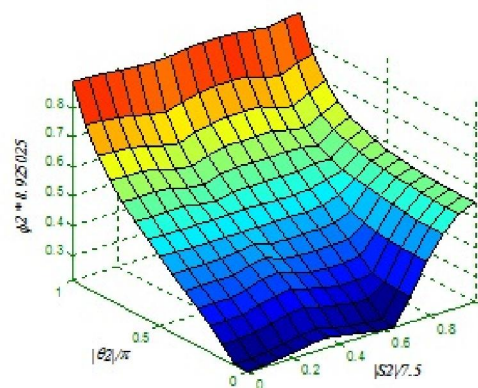
(a)



(b)

	<i>Input</i>   $S_2$			
	Z	M	B	
<i>Input</i>   $\theta_2$	Z	1	1	2
	M	1	1	2
	B	3	3	3

(c)



(d)

Fig.12. (a) The design of number and Rule-Bases of FLC.1. (b) Fuzzy 3<sup>rd</sup> plot Inputs  $|S_1|$  &  $|\theta_1|$  and Output  $\varphi_1$ . (c) The design of number and Rule-Bases of FLC.2. (d) Fuzzy 3<sup>rd</sup> plot inputs  $|S_2|$  &  $|\theta_2|$  and Output  $\varphi_2$ .

Where in Fig.12 (a), 1 is Zero,2 is Small, 3 is Medium, 4 is Big and 5 is Very Big. Similarly, Fig.12 (c), 1 indicates Zero, 2 is Medium and 3 is Very Big. And the

number of rule-bases and rule-bases for GAIN are achieved as below:

- (R1) IF T is Zero THEN Q is Zero
- (R2) IF T is Very Small THEN Q is Very Small
- (R3) IF T is Small THEN Q is Small
- (R4) IF T is Medium THEN Q is Medium
- (R5) IF T is Big THEN Q is Big
- (R6) IF T is Very Big THEN Q is Very Big

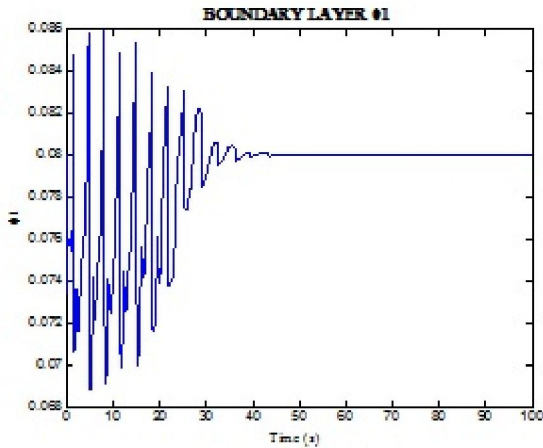


Fig.13. Time varying boundary layer thickness  $\phi_1$ , Point C

Fig.14. Time varying boundary layer thickness  $\phi_2$ , Point C

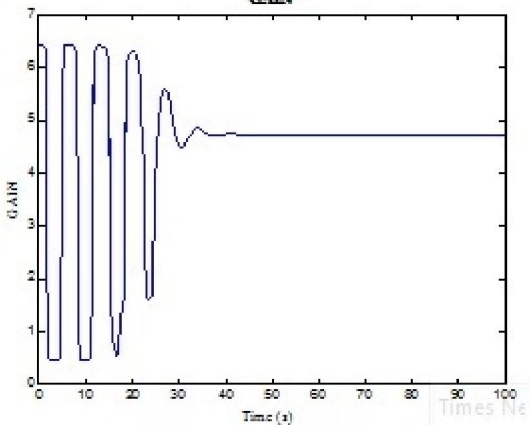
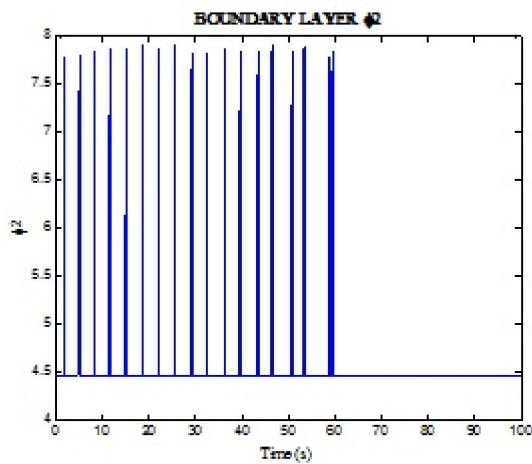


Fig.15. Fuzzy Gain of (32), Point C

For point C of Pareto set, the CART position and Pole position for time varying boundary layer thickness TORA system are achieved as Fig.16 and Fig.17, respectively.

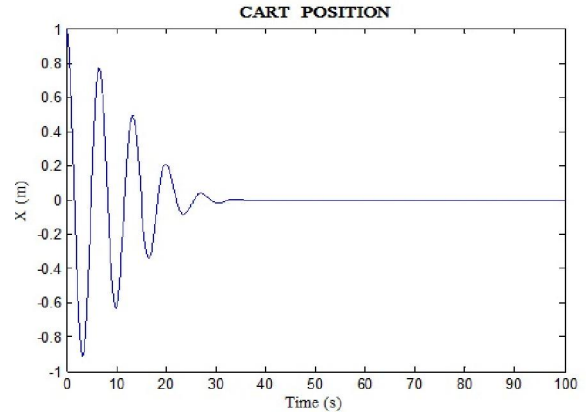


Fig.16. CART position time varying boundary layer, point C

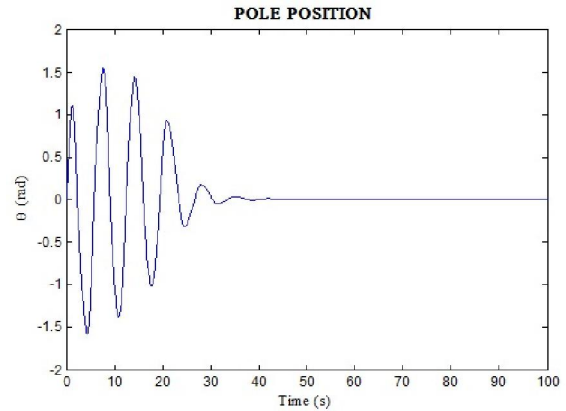


Fig.17. Rotation Actuator position time varying boundary layer, point C

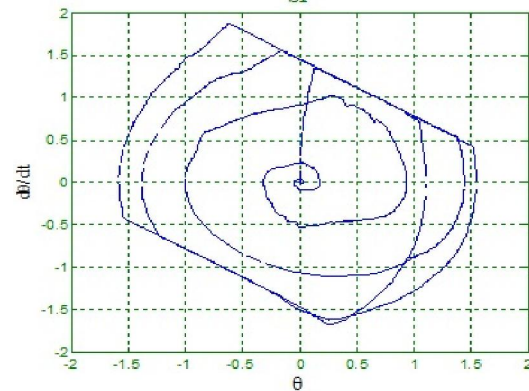


Fig. 18. Dynamic motion during phase plane by mandatory Moving Switching surface motion (Time varying Boundary layer Thickness)

Corresponding Fig. 18 and attention to trajectory implies this fact that linear motion trajectory strikes when the MSS surface is stopped. Apposite rapid trajectory implies the precipitation of fast motion of MSS in the phase plane. In fact, this kind of surface motion is impressible of variation of boundary layer upon the constant surface  $S_2$ , which has a measurement surface or base surface in the DSMC strategy.

4.6. TORA system and constant boundary layers

Comparing the constant boundary layer thickness in contrast to time varying boundary layer thickness in TORA system to illustrate the behavior of this system with constant boundary layer, assume the parameters of DSMC [ (C<sub>1</sub>, C<sub>2</sub>, Z<sub>u</sub>) section.4] in point C of Pareto set. And maximum of boundary layers [6],  $\varphi_{1max} = 0.08593$ ,  $\varphi_{2max} = 7.9138$ , (Fig.22,23) and  $\eta \geq 10.0$  ( $\eta \geq K_{max}\beta/C_1$  condition) substituting in (28) and  $t_s = 0.05$ . The CART position and POLE position are achieved as Fig. 19 and Fig. 20, respectively. Table 3 illustrates the comparison of settling time for point C of time varying boundary layer thickness and constant boundary layer thickness for CART position and POLE position.

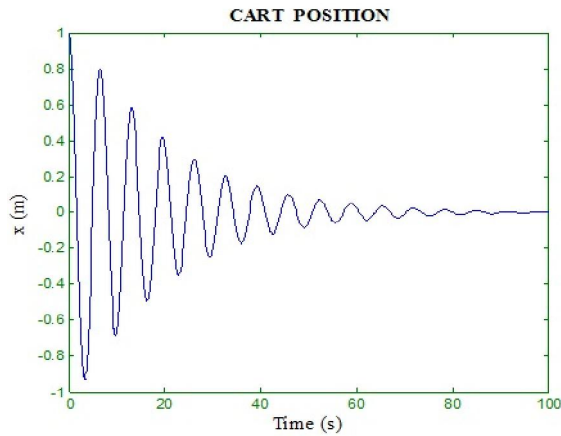


Fig.19. CART position, constant boundary layer thickness

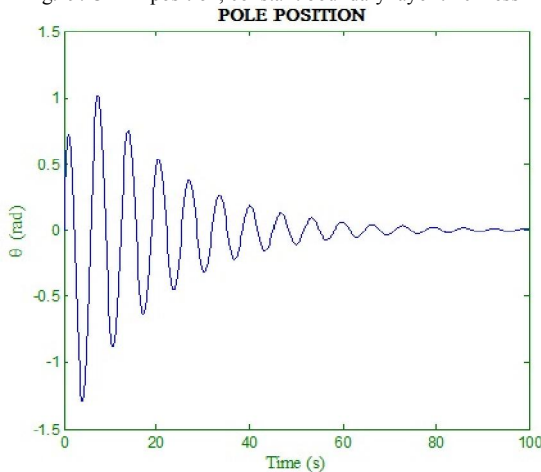


Fig.20. POLE position, constant boundary layer thickness

Comparing the results and solution between the time varying boundary layer thickness and constant boundary, the stability and robustness is strongly demonstrated (Fig. 16, 17, 19 and 20). During the time-starting of the system, the tracking error in constant boundary layer is a little better. This event is impressive of the constrained motion of MSS. This means while the system trajectory is trying to reach the MSS, the convergence and reaching this surface with respect to the fast variation of surface is almost hard. In addition, as we expect, the results of time-varying boundary layer thickness are more preferable than the constant boundary layer thickness from robustness and tracking-error point of view.

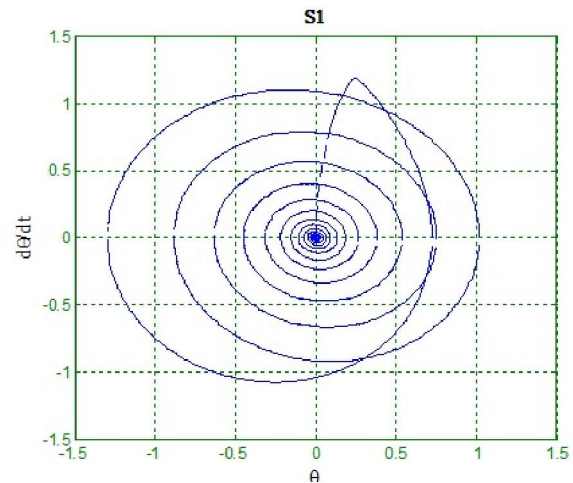


Fig. 21. Dynamic motion during phase plane by natural Moving Switching Surface motion (Constant Boundary layer Thickness)

Fig.21, demonstrates the trajectory of a dynamic system with natural Motion of MSS in the phase plane with a constant boundary layer thickness on Base constant surface  $S_2$ .

Table 3: Comparison of settling time, constant and time varying boundary layer, for TORA system

TORA system	CART position Settling Time(s)	POLE Position Settling Time(s)
Time Varying Boundary Layer (Point C)	24.61	29.91
Constant Boundary Layer	58.85	63.50

**References:**

- [1] Young, K. K. D., Kokotovic, P. V., and Utkin, V. I., 1977, A singular perturbation analysis of high-gain feedback systems. *IEEE Transactions on Automatic Control*, 22, 931-938.
- [2] Choi, S. B., Cheong, C.C. and Park, D. W, *Moving Switching Surface for robust control of second-order variable structure systems*. International Journal of control 58.,1993, pp.229-45.
- [3] Bartoszowicz, A. 1995: *A Comment on ' A time varying sliding surface for fast and robust tracking control of second-order uncertain systems'*, *Automatica* 31, 1893-95.
- [4] Bartoszewicz, A. 1996: Time-varying sliding modes for second-order systems. *IEE Proceeding of Control Theory Application* 143, 455-62.
- [5] H. Lee, E. Kim, H. J. Kang, M. Park: *A new sliding-mode control with fuzzy boundary layer*. *Fuzzy Sets and Systems* 120(2001) 135-143.
- [6] J. J. Slotine, W. Li, *Applide Nonlinear Control*, Printice-Hall, Engelwood Cliffs, NJ, 1991.
- [32] L. C. Hung, H. Y. Chang, *Decouple sliding-mode with fuzzy-neural network controller for nonlinear systems*, *International Journal of Approximate Reasoning* 46(2007) 74-97.
- [7] L. A. Zadeh, "Fuzzy Sets", *Inf. Contr.*, vol.21, pp.338-353, 1965.
- [8] E. H. Mamdani and S. Assilian, "An experiment in linguistic synthesis with fuzzy logic controller," *Int. J. Man-Mach. Stud.*, vol. 7, no.1,pp. 1-13, 1975.
- [9] B. Kosko, *Neural Networks and Fuzzy Systems*. Englewood Cliffs, NJ: Prentice- Hall, 1992.
- [10] R. Jang, "Self-learning fuzzy controllers based on temporal back propagation," *IEEE Trans. Neural Networks*, vol. no.5, pp.714-723, 1992.
- [11] C. Karr. "Genetic algorithm for fuzzy controllers," *AI Expert*, vol.6,pp.26-33, Feb. 1991.
- [12] D.T. Pham and D. Karaboga, "Optimum design of fuzzy logic controllers using genetic algorithms," *J. Syst. Eng.*, vol. 1, no.2, pp. 114-118, 1991.
- [13] A. Homaifar and E. McCormick," *Full design of fuzzy controllers using genetic algorithm*," in *SPIE Vol.1766-Neural and Stochastic Methods in Image and Signal Processing*, 1992, pp. 393-404.
- [14] M. A. Lee and H. Takagi, "Integrating design stages of fuzzy systems using genetic algorithms," in *Proc. 2<sup>nd</sup> IEEE Int. Conf. Fuzzy Syst.*,1993, pp.612-617.
- [15] K. C. Ng and Y. Li, "Design of sophisticated fuzzy logic controllers using genetic algorithms," in *Proc. 3<sup>rd</sup> IEEE Int. Conf. Fuzzy Systems*, 1994, pp. 1708-1712.
- [16] M. G. Cooper, "Evolving a rule-based fuzzy controller," *Simulation*, Vol. 65, no.1, pp. 67-73, 1995.
- [17] D. A. Linkens and H. O. Nyonggesa, "Genetic algorithms for fuzzy control- Part I: Offline system development and application," *Proc. Inst. Elect. Eng. Contr. Theory Applicat.*, Vol. 142, pp. 161-176, May 1995.
- [18] D. A. Linkens and H. O. Nyonggesa, "Genetic algorithms for fuzzy control- Part 2: Online system development and application," *Proc. Inst. Elect. Eng. Contr. Theory Applicat.*, Vol. 142, pp.177-185, May 1995.
- [19] J. H. Holland, *Adaptation in natural and Artificial Systems*, Ann Arbor, MI: Michigan Press, 1975.
- [20] Arora, J. S., *Introduction to Optimum Design*, 1989 (Mc Graw-Hill: Singapore).
- [21] Sarker, R., Liang, K.-H. and Newton, C., A new continuous optimization multiobjective evolutionary algorithm. *Eur. J. Oper. Res.*, 2002, 140, 12-23.
- [22] Rao, S. S., *Engineering Optimization Theory and Practice*, 1996 (John Wiley & Sons: NY).
- [23] Renner, G and Ekart, A., *Genetic algorithms in Computer aided design*. *Comput. Aided Des.*, 2003, 35, 709-726.
- [24] Fonseca C. M. and Fleming, P. J., *Genetic algorithms for multi-objective optimization: Formulation, discussion and generalization*. *Proceedings of the Fifth International Conference on Genetic Algorithms*, edited by S.

- Forrest (San Mateo CA) 416-423, 1994, 2(3), 221-248.
- [25] Srinivas, N. and Deb, K., *Multi-objective optimization using nondominated sorting in genetic algorithms*. *Evol. Comput.*, 1994, 2(3), 221-248.
- [26] Coello Coello, C. A. and Christiansen, A. D., *Multi objective optimization of trusses using genetic algorithms*. *Comput. Struct.*, 2000, 75, 647-660.
- [27] Coello Coello, C. A., Van Veldhuizen, D. A. and Lamont, G. B., *Evolutionary Algorithms for Solving Multi-objective Problems*, 2002 (Kluwer Academic Publishers; New York).
- [28] Deb, K., Agrawal, S., Pratap. A. and Meyarivan, T., " *A fast and elitist multi-objective genetic algorithm: NSGA-II* ", *IEEE Trans. On Evolutionary Computation* 6(2): 182-197, 2002.
- [29] Lee.Zing. Wang, Da.Ruan, E.Kerre, *A course in Fuzzy systems and control*, Prentice Hall PTR, 1997.
- [30] Cheong, F., Lai, R., *Constraining the Optimization of Fuzzy Logic Controller Using an Enhanced Genetic Algorithm*, *IEEE Transactions on Systems, Man and Cybernetics-Part B: Cybernetics*, vol 30, No.1, Feb 2000.
- [31] P. J. Mac Vicar-Whelan, "Fuzzy sets for man-machine interaction," *Int. J. Man-Mach. Stud.*, vol.8, pp.687-697, 1976.
- [32] Park, Y. J., Cho, H. S., D. H., *Genetic Algorithm-Based Optimization of Fuzzy Logic Controller Using Characteristic Parameters*, *Proceedings of the 1995 IEEE International Conference on Evolutionary Computation*, pp.831-836.
- [33] Z. Michalewicz, *Genetic Algorithm+Data Structures=Evolution Programs*. New York: Springer-Verlag, 1992.

6/24/2014